Geophysical Research Letters

RESEARCH LETTER
10.1029/2026GL123015

Late Carboniferous Paleomagnetism From North Qiangtang Block Reveals a Multibranched Paleo-Tethys Ocean

Jiahui Zhang[1], Xin Cheng[1], Zhongshan Shen[2], Daniel Pastor-Galán[3,4], Bitian Wei[2], Longyun Xing[1], Dongmeng Zhang[1], Nan Jiang[5], Mengting Zhong[1], Shuqi Lan[1], Muhammad Rizwan[1], Chenglong Deng[2], and Hanning Wu[1]

[1]State Key Laboratory of Continental Evolution and Early Life, Department of Geology, Northwest University, Xi'an, China, [2]State Key Laboratory of Lithospheric and Environmental Coevolution, Institute of Geology and Geophysics, Chinese Academy of Sciences, Beijing, China, [3]Instituto de Geociencias (IGEO), CSIC, Madrid, Spain, [4]Frontier Research Institute for Interdisciplinary Sciences, Tohoku University, Sendai, Japan, [5]School of Petroleum Engineering and Environmental Engineering, Yan'an University, Yan'an, China

Abstract The North Qiangtang Block occupies a pivotal position within the eastern Tethyan realm, and its paleogeographic reconstruction is critical for constraining Tethyan geometry and evolution. However, its Late Paleozoic paleogeography and Paleo-Tethyan Ocean–continent configuration remain controversial due to limited reliable age-constrained paleomagnetic data. Here we present paleomagnetic and geochronological data from Late Carboniferous limestones of the Walongshan Formation, providing an absolute-age-constrained paleomagnetic pole. Stepwise demagnetization of 126 specimens from 19 sites isolated a pre-folding characteristic remanent magnetization carried by magnetite, indicating a paleolatitude of 19.5 ± 5.2°S at 317 ± 11.6 Ma. Together with published paleomagnetic and geologic constraints, these results suggest that the North Qiangtang–Indochina "central continental domain" remained at middle to low latitudes in the Southern Hemisphere from the Late Carboniferous to the Middle Permian, favoring a dual-branch Paleo-Tethys configuration with a northern Jinshajiang oceanic basin (~5,500 km) and a southern Longmu Co–Shuanghu oceanic basin (~3,300 km).

Plain Language Summary Reconstructing the ocean–continent distribution pattern within the Tethyan realm during the Late Paleozoic requires reliable, well-dated information about where key continental blocks were located. The position of the North Qiangtang Block on the Tibetan Plateau has been uncertain, leading to different reconstructions of how the Paleo-Tethys Ocean and nearby continents were arranged. We studied the magnetic record preserved in Late Carboniferous limestones of the Walongshan Formation and combined it with age information. The rocks retain an original magnetic signal, carried mainly by magnetite, that formed before the layers were folded. This signal indicates that the North Qiangtang Block lay at about 20° south latitude around 317 million years ago. Combined with previous geological and paleomagnetic evidence, our results support a picture in which North Qiangtang and Indochina formed a central belt of continent between two ocean basins: the Jinshajiang oceanic basin to the north (~5,500 km) and the Longmu Co–Shuanghu oceanic basin to the south (~3,300 km).

Key Points:

- The North Qiangtang Block was located at 19.5 ± 5.2°S at 317 ± 11.6 Ma
- The North Qiangtang–Indochina domain occupied mid-to-low latitudes in the Southern Hemisphere during the Late Carboniferous–Middle Permian
- During the Late Carboniferous, the Jinshajiang and Longmu Co–Shuanghu oceanic basins formed a dual-branch Paleo-Tethys Ocean

Supporting Information:

Supporting Information may be found in the online version of this article.

Correspondence to:

X. Cheng and Z. Shen,
chengxin@nwu.edu.cn;
zsshen@mail.iggcas.ac.cn

Citation:

Zhang, J., Cheng, X., Shen, Z., Pastor-Galán, D., Wei, B., Xing, L., et al. (2026). Late Carboniferous paleomagnetism from North Qiangtang Block reveals a multibranched Paleo-Tethys Ocean. *Geophysical Research Letters*, *53*, e2026GL123015. https://doi.org/10.1029/2026GL123015

Received 15 MAR 2026
Accepted 26 MAY 2026

Author Contributions:

Conceptualization: Jiahui Zhang, Xin Cheng, Zhongshan Shen, Hanning Wu
Data curation: Jiahui Zhang, Bitian Wei
Formal analysis: Jiahui Zhang, Xin Cheng, Zhongshan Shen
Funding acquisition: Xin Cheng, Chenglong Deng, Hanning Wu
Investigation: Jiahui Zhang, Xin Cheng, Longyun Xing, Dongmeng Zhang, Nan Jiang, Mengting Zhong, Shuqi Lan, Muhammad Rizwan
Methodology: Jiahui Zhang, Xin Cheng, Bitian Wei, Longyun Xing

1. Introduction

During the Late Paleozoic, the global tectonic framework underwent significant restructuring as northern Laurasia and southern Gondwana gradually converged and ultimately amalgamated into the Pangean supercontinent (Domeier & Torsvik, 2014; Pastor-Galán, 2022). The Paleo-Tethys Ocean, situated between Laurasia and Gondwana, acted as a pivotal geodynamic nexus. While it is widely accepted that the Paleo-Tethys Ocean was fully formed by the Late Carboniferous, debates persist regarding its geometry and tectonic nature (Pastor-Galán et al., 2025; Zhao et al., 2018). One view proposes that the Paleo-Tethys Ocean constituted a single continuous oceanic basin (Golonka & Ford, 2000; Guan, Liu, et al., 2021; Zhang et al., 2022), whereas other views suggest that it comprised multiple coeval oceanic branches, the most prominent of which were the southern Longmu Co–Shuanghu Ocean and the northern Jinshajiang Ocean (Cheng et al., 2024; Wei et al., 2023, 2025; Zhao et al., 2018). Therefore, constraining the spatial configuration of the Paleo-Tethys Ocean is crucial not only for reconstructing its evolutionary history but also for elucidating rift dynamics along the northern margin of

Project administration: Xin Cheng, Chenglong Deng
Software: Jiahui Zhang, Bitian Wei
Supervision: Xin Cheng, Zhongshan Shen, Chenglong Deng, Hanning Wu
Validation: Jiahui Zhang
Visualization: Bitian Wei
Writing – original draft: Jiahui Zhang
Writing – review & editing: Jiahui Zhang, Xin Cheng, Zhongshan Shen, Daniel Pastor-Galán, Bitian Wei, Chenglong Deng, Hanning Wu

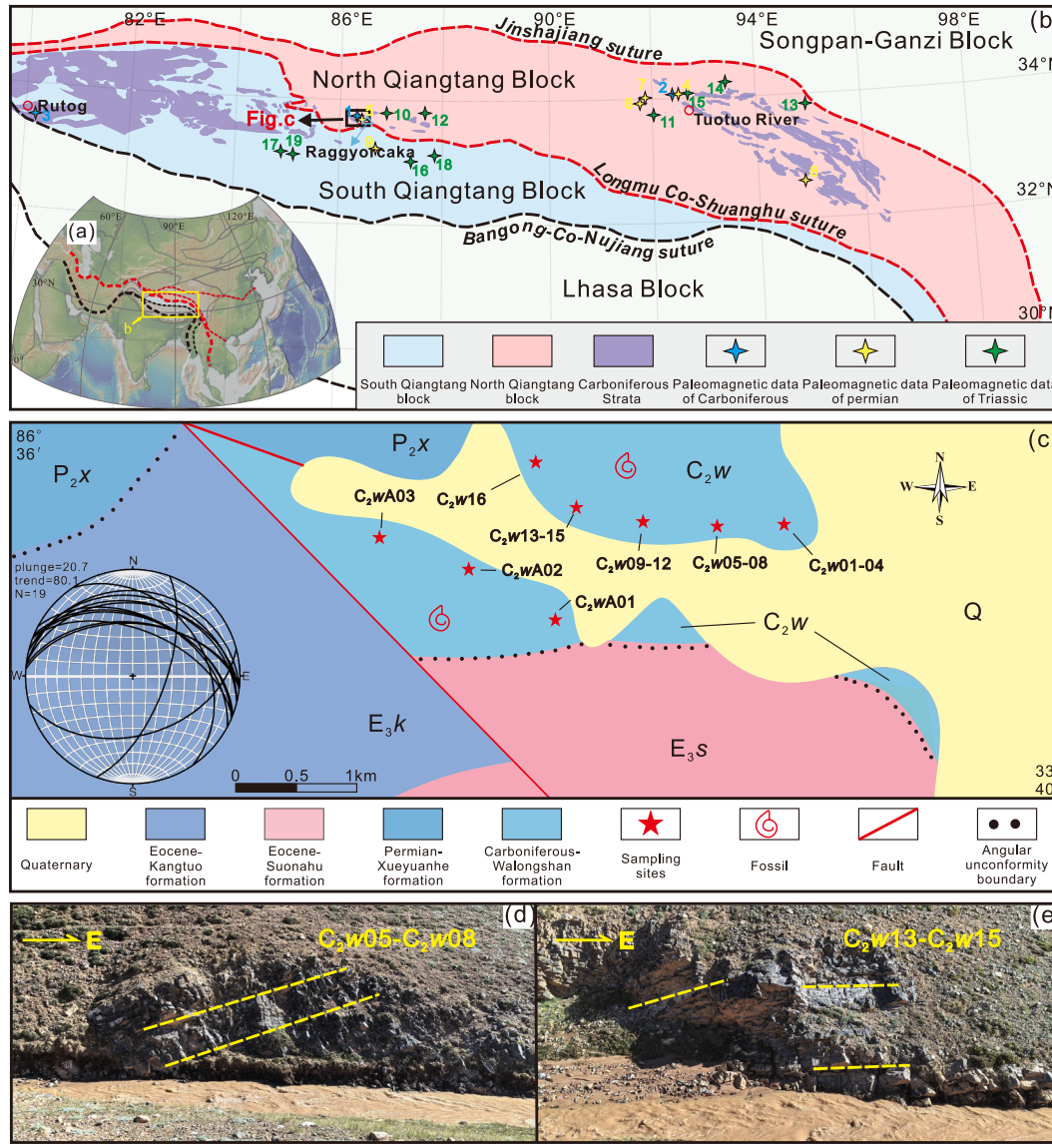

Figure 1. (a) Location map of the Tibetan Plateau and the Qiangtang Block (modified after Wei et al., 2023); (b) Distribution of Carboniferous strata in the Qiangtang Block and locations of published paleomagnetic studies. Numbers correspond to references: 1 Cheng et al. (2012); 2 Yang et al. (2017); 3 Cheng et al. (2013); 4 Song et al. (2017); 5 Cheng et al. (2012); 6 Cheng et al. (2024); 7 Ma et al. (2019); 8 Guan, Yan, et al. (2021); 9 Wei et al. (2022); 10 Zhou et al. (2019); 11 Song et al. (2020); 12 Song et al. (2012); 13 Yu et al. (2022); 14 Lin and Watts. (1988); 15 Song et al. (2015); 16 Song et al. (2012); 17 Wei et al. (2025); 18 Ma et al. (2024); 19 Ma, Tan, et al. (2025); (c) Geological map of the sampling area (modified from JUIGS, 2006) with an inset equal-area stereographic projection of bedding attitudes showing an overall E–W-trending fold axis with a trend/plunge of 80.1°/20.7°; (d)–(e) Field photos of the sampling section.

Gondwana and the geodynamic processes governing Pangea amalgamation (Torsvik & Cocks, 2017; Wu et al., 2020).

The Qiangtang Block, situated in the central part of the Tibetan Plateau (Figure 1a), is a key tectonic unit that preserves complete geologic records of the Paleo-Tethys Ocean's evolution (Wu et al., 2020; Zhu et al., 2022). Traditionally, the Qiangtang Block has been regarded as a unified continental block derived from the Pan-African basement of Gondwana (Kapp et al., 2003; Pullen et al., 2008; Zhang et al., 2022). During the Late Paleozoic, the Qiangtang Block, together with other Cimmerian blocks, rifted from the northern margin of Gondwana and subsequently drifted northward (Angiolini et al., 2013; Song et al., 2017). The Paleo-Tethys Ocean ultimately closed as these blocks collided with and were accreted to the southern margin of Eurasia (Pullen et al., 2008;

Wang et al., 2018; Xu et al., 2015). However, recent advances in geology, stratigraphy, and paleomagnetism increasingly challenge this hypothesis. Growing evidence indicates that the Qiangtang Block is not tectonically coherent but instead comprises two distinct sub-blocks—the North Qiangtang Block (NQB) and the South Qiangtang Block (SQB)—separated by the Longmu Co–Shuanghu Suture Zone (Wei et al., 2025; Zhai et al., 2011). The Longmu Co–Shuanghu Suture Zone is widely interpreted to record subduction and closure of an oceanic basin of unknown size, known as the Longmu Co–Shuanghu Ocean. Within this revised framework, the Paleo-Tethys Ocean is best regarded as a multi-branched oceanic system. Therefore, constraining the Late Paleozoic paleogeographic position of the NQB is crucial for reconstructing the paleogeography of the Paleo-Tethys Ocean.

Paleomagnetism provides quantitative constraints on paleolatitude and thus on the paleogeographic positions and drift histories of tectonic blocks. Recent paleomagnetic studies of Tibetan blocks have advanced rapidly, offering new constraints on the NQB and SQB and on Paleo-Tethys evolution (Cheng et al., 2024; Song et al., 2017; Wei et al., 2022, 2025). However, currently available reliable paleomagnetic data are still concentrated mainly in Permian and younger strata. Collectively, these results depict a "one-way train" style evolutionary history in which the NQB drifted continuously northward from the Southern Hemisphere and eventually amalgamated with Eurasia. By contrast, reliably time-anchored pre-Permian paleomagnetic constraints remain scarce (Jiang et al., 2022; Yang et al., 2017). Here we present paleomagnetic results from Late Carboniferous limestones of the Walongshan Formation in the Raggyorcaka area, integrated with in situ LA-ICP-MS U-Pb dating of syn-sedimentary calcite. We further synthesize regional geological, geochemical, and paleontological evidence to constrain tectonic relationships between the NQB and adjacent blocks and to evaluate the geometry and evolution of the Paleo-Tethys Ocean.

2. Geological Setting and Sampling

Carboniferous strata are sparsely exposed within the Qiangtang Block (Hu et al., 2024). The outcrops are mainly distributed in the western SQB (e.g., the Rutog area) and in the central (e.g., the Raggyorcaka area) and eastern (e.g., the Tuotuo River area) NQB (Figure 1b). The small and discontinuous nature of these outcrops means that our understanding of Carboniferous stratigraphic architecture, sedimentary systems, and tectonic evolution in the NQB remains fragmentary. The Raggyorcaka area preserves well-exposed Carboniferous–Permian strata of the NQB (Cheng et al., 2006; Xie et al., 2025; Zhang et al., 2016) and is an ideal area for investigating its Late Paleozoic geological record.

Our field investigation focuses on Carboniferous strata in the Raggyorcaka area, Nyima County (Figure 1b). The Walongshan Formation occurs in small, discontinuous outcrops and comprises a lower carbonate-dominated unit and an upper siliciclastic-rich unit (Hu et al., 2024). Fossils are abundant, with corals and brachiopods in the lower unit and fusulinid larger benthic foraminifers (notably *Fusuliella* and *Pseudostaffella*) in the upper unit, consistent with warm-water, shallow-marine carbonate platform-to-ramp deposition during the Late Carboniferous (Cheng et al., 2006; Zhang et al., 2021). Biostratigraphic constraints place the Walongshan Formation in a rather long Serpukhovian–Gzhelian interval (~330–300 Ma) (Cheng et al., 2006; Hu et al., 2024; Zhang et al., 2021). Structural relationships indicate that the principal folding affecting the Walongshan Formation predates the Late Triassic and may have been related to tectonic reorganization during Paleo-Tethyan closure: Upper Triassic Nadigangri volcanic rocks unconformably overlie already folded Middle–Upper Triassic strata, whereas Late Triassic intrusions are essentially undeformed (Zhai & Li et al., 2007). Although minor younger overprinting related to post-collisional shortening following the India–Asia collision cannot be excluded, the bedding attitudes define an overall E–W-trending fold axis with a plunge of ~20.7°, suggesting that later deformation did not significantly modify the regional fold-axis orientation.

For paleomagnetic sampling, we collected 150 independently oriented cores from 19 sites (6–10 per site) spanning multiple stratigraphic levels of the Walongshan Formation limestone succession. We additionally collected two limestone samples for in situ U–Pb dating of syndepositional calcite matrix to further constrain the depositional age of the Walongshan Formation. Details of the regional geology, site locations, bedding attitudes, and sampling procedures are provided in Text S1 in Supporting Information S1.

3. Results

Methodological details for calcite U–Pb dating, petrography, rock-magnetic measurements, and paleomagnetic procedures are provided in Text S2 in Supporting Information S1, and the corresponding results are presented in Texts S3–S6, covering petrography (Text S3 and Figure S1 in Supporting Information S1), calcite U–Pb geochronology (Text S4 and Figure S2 in Supporting Information S1), rock magnetism (Text S5 and Figures S3–S4 in Supporting Information S1), and paleomagnetism (Text S6 in Supporting Information S1). In situ U–Pb dating of syndepositional calcite constrains deposition of the Walongshan Formation to ca. 324–311 Ma, consistent with fossil-based biostratigraphic constraints (Figure S2, Cheng et al., 2006; Zhang et al., 2021). Optical microscopy and SEM–EDS observations show that the samples are dominated by calcite and display little evidence for metamorphism or extensive diagenetic/hydrothermal alteration. Iron-oxide magnetic grains are also well preserved (Figure S1 in Supporting Information S1). Together with rock-magnetic experiments, these observations indicate that magnetite is the dominant magnetic carrier in the Walongshan Formation limestones (Figures S3–S4 in Supporting Information S1).

Of the 150 independently oriented cores collected from 19 sites, 126 specimens yielded stable ChRM components upon stepwise demagnetization. The ChRM component data for individual specimens are provided in Table S5 in Supporting Information S1. Most Walongshan Formation limestone specimens exhibit a two-component demagnetization behavior (Figures 2a–2d): a low-temperature component is removed below ~300–330°C, whereas a high-temperature (or high-coercivity) component is typically unblocked between ~330°C and 475–500°C (or up to 60 mT) and is interpreted as the characteristic remanent magnetization (ChRM). ChRM directions obtained from thermal and hybrid demagnetization are highly consistent (Figures 2c and 2d), further supporting the reproducibility of the ChRM directions.

A stable ChRM was isolated at all 19 sites (Table S3 in Supporting Information S1). In situ (geographic) site-mean directions are $D_g = 223.9°$, $I_g = 4.4°$, $k_g = 13.2$, and $\alpha_{95g} = 9.6°$. In tilt-corrected (stratigraphic) coordinates, the mean is $D_s = 223.9°$, $I_s = 34.8°$, $k_s = 40.0$, and $\alpha_{95s} = 5.4°$ (Figures 2g and 2h). Considering the possible effects of local vertical-axis rotations and non-ideal fold geometry in the study area, we applied multiple fold tests to constrain the timing of remanence acquisition from complementary statistical and structural perspectives. This component passes the fold test at the 99% confidence level (McElhinny, 1964), with maximum grouping at 93.5 ± 8.1% unfolding (Figure 2j; Watson & Enkin, 1993), and this interpretation is further supported by the Enkin (2003), McFadden (1990), inclination-only (Ma, Hu, et al., 2025), and bootstrap fold tests (Figure S5 in Supporting Information S1; Tauxe et al., 2016). To further evaluate the potential influence of fold-axis plunge, we performed a double structural correction; the resulting plunge-corrected tilt-corrected mean direction is $D_s = 227.4°$, $I_s = 34.5°$, $k = 37.8$, and $\alpha_{95} = 5.5°$ (Figure S7 and Table S6 in Supporting Information S1), which is consistent with the conventional tilt-corrected direction within uncertainty and indicates that fold-axis plunge did not significantly affect the ChRM direction. In addition, 45° IRM tests (Figure S6 in Supporting Information S1) yield slopes close to unity over 350–560°C (factor = IRM_Z/IRM_X = 0.911–1.038), suggesting little to no inclination shallowing and therefore accurate paleolatitude estimates.

After converting the mean directions of the 19 sites into virtual geomagnetic poles, we obtain a corresponding paleomagnetic pole at $P_{lat.} = -22.4°$N, $P_{long.} = 41.8°$E, $A_{95} = 5.2°$. This pole corresponds to a Late Carboniferous paleolatitude of 19.5 ± 5.2°S for the North Qiangtang Block (reference point: 33.7°N, 86.7°E).

4. Nature of the Magnetization

In situ U–Pb dating of calcite matrix from Walongshan Formation limestones yields a weighted mean age of 317 ± 11.6 Ma, consistent with a Late Carboniferous age independently inferred from Serpukhovian–Gzhelian faunal assemblages (~330–300 Ma; Hu et al., 2024). Within this age framework, we evaluate whether the ChRM is (pseudo-)primary.

The Walongshan Formation limestones were sampled from two stratigraphic sections, and site-mean ChRM directions pass fold tests (Figure 2j). After tilt correction of 19 site-mean directions, the Fisher precision parameter increases from 13.2 to 40.0 and α95 decreases from 9.6° to 5.4°, indicating significantly improved clustering in tilt-corrected coordinates (Figures 2g and 2h). These results show that the ChRM predates bedding tilt and is therefore pre-tectonic. All ChRM directions are of reversed polarity, consistent with a Late Carboniferous age within the Kiaman Reversed Superchron (Cottrell et al., 2008). Together, the fold tests and polarity

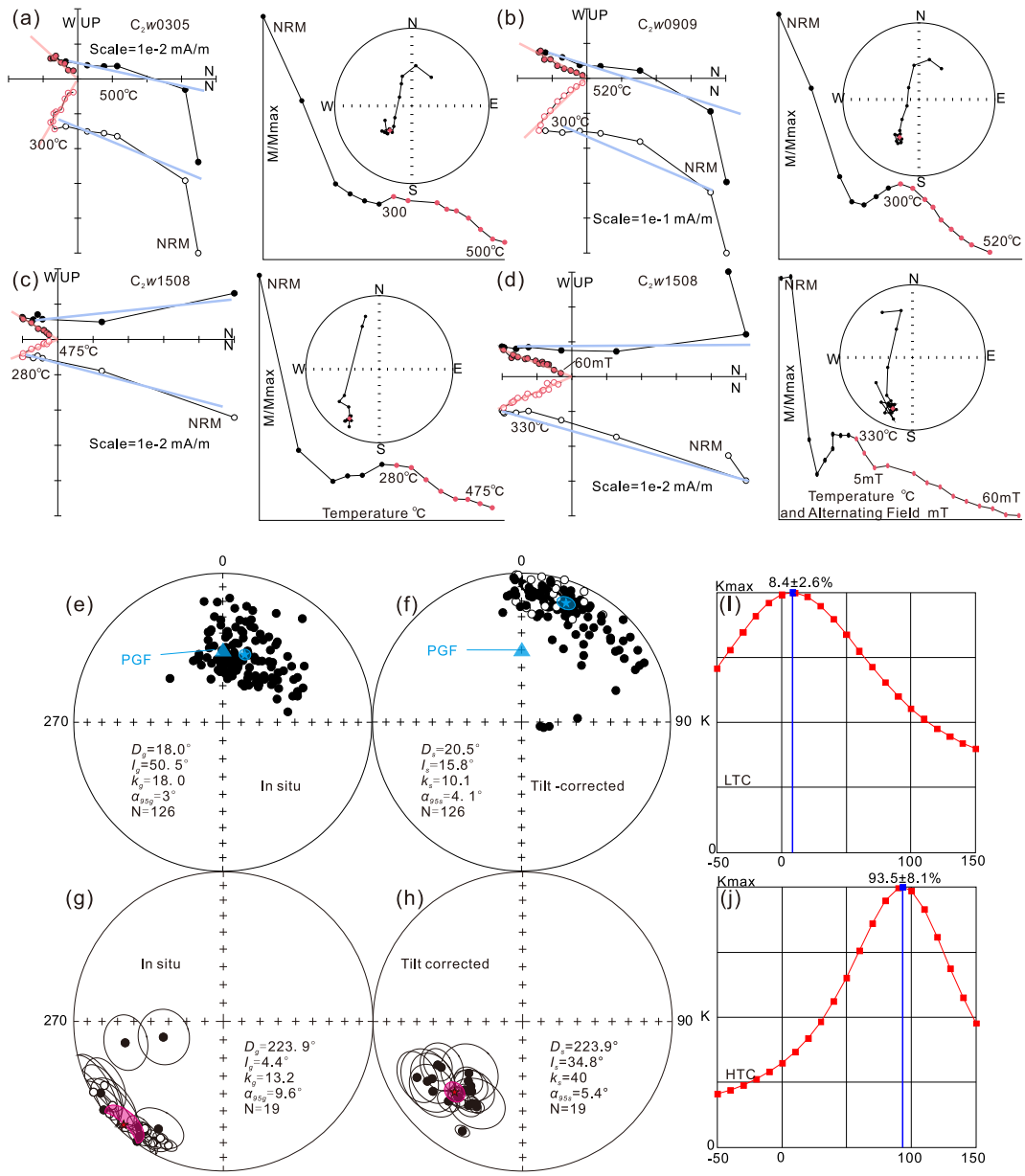

Figure 2. (a–d) Representative demagnetization behavior of Walongshan Formation samples shown in stratigraphic (tilt-corrected) coordinates. (e–f) Equal-area projections of specimen-level LTC directions before and after tilt correction. (g–h) Equal-area projections of site-mean HTC directions before and after tilt correction. The cyan symbol indicates the expected present geomagnetic field (PGF) direction at the sampling site. Open (filled) symbols represent upper- (lower-) hemisphere projections. (i–j) Incremental unfolding tests for the LTC and HTC (Watson & Enkin, 1993).

data support a pre-tectonic magnetization and provide the basis for further evaluating its primary origin using rock-magnetic and microtextural evidence.

In carbonate rocks from regions lacking significant thermal anomalies, the preservation of a primary ChRM depends on the relative contributions of detrital or biogenic magnetic carriers and magnetic minerals formed during late diagenesis. Widespread chemical remagnetization in unmetamorphosed carbonates has commonly been linked to late-diagenetic authigenic magnetite, which is typically characterized by wasp-waisted hysteresis loops, predominantly superparamagnetic–stable single-domain grain-size distributions, and Day-plot trends consistent with superparamagnetic and single-domain/pseudo-single-domain mixing curves (e.g., Fabian, 2003; Yao et al., 2024). By contrast, the Walongshan limestones show a magnetic assemblage dominated by pseudo-

single-domain magnetite: hysteresis loops lack pronounced wasp-waisted shapes, FORC diagrams show no diagnostic SP features, and Day-plot data from 18 representative specimens cluster mainly in the PSD field and extend toward the SD–MD transition (B_{cr}/B_c = 2.70–5.67, mean = 4.16; M_{rs}/M_s = 0.054–0.137, mean = 0.097; Figure S4 and Table S2 in Supporting Information S1). These results indicate that stable remanence is carried mainly by PSD–MD magnetite and argue against late-diagenetic authigenic magnetite as the dominant carrier. Consistently, the Walongshan data plot away from published remagnetized carbonate data sets and overlap with fields defined by carbonates carrying primary magnetizations (Jackson & Swanson-Hysell, 2012; Fu et al., 2022; Yu et al., 2022; Yao et al., 2024; Figure S4 in Supporting Information S1).

Formation of authigenic magnetic minerals during late diagenesis is commonly associated with fluid circulation (Dekkers, 2012; Elmore et al., 2012; Pastor-Galán et al., 2016). Optical microscopy reveals no evidence of metamorphism, significant chemical alteration, or pervasive late-stage veining, and secondary mineral phases are rare. SEM images show magnetic grains with sharp boundaries against the surrounding matrix and no oxidation rims or fracture-related infillings. These microtextural features are inconsistent with pervasive late-diagenetic authigenic growth and are more compatible with a detrital origin.

Moreover, comparison with a compilation of reliable Late Carboniferous to Late Triassic paleomagnetic poles for the NQB ($R \geq 5$; Table S4 in Supporting Information S1) shows that our new pole is distinct from most published NQB poles younger than the Late Carboniferous (Figure 3a), further supporting a primary origin for the ChRM. Taken together, these independent lines of evidence support a primary remanence interpretation, and our data set satisfies six of the seven primary benchmarks of the R-score reliability criteria (Meert et al., 2020; Text S7 in Supporting Information S1). We therefore interpret this new age-constrained paleomagnetic result as recording primary remanence acquired during deposition at ca. 317 ± 11.6 Ma, placing the North Qiangtang Block at 19.5 ± 5.2°S in the Late Carboniferous.

5. Late Carboniferous Paleogeography of the NQB

To evaluate the tectonic implications of the newly constrained Late Carboniferous paleolatitude and inferred drift history of the NQB (Figures 3b and 3c), we re-evaluated published paleomagnetic constraints from the NQB and adjacent blocks, including the SQB and Indochina Block (IC). Data screening followed the seven reliability criteria of Meert et al. (2020), and only data sets with R ≥ 5 were retained (Table S4 in Supporting Information S1). For the South China Block, North China Block, Tarim Block, and the India plate, we adopted APW reference poles from previously published APW paths based on high-quality paleomagnetic data sets (Table S4 in Supporting Information S1; Huang et al., 2018; Vaes et al., 2023).

Given the long-standing debate over Late Paleozoic Pangean configurations, particularly the relative fit between Laurussia and Gondwana, we briefly review the competing models here. Previous paleomagnetic studies have shown that direct application of the classical Pangea A configuration to Late Carboniferous–Early Permian reconstructions may produce substantial geometric overlap between Laurussia and Gondwana (Domeier et al., 2012; Torsvik et al., 2012). To address this mismatch, subsequent studies proposed the Pangea B model, which requires a greater lateral offset of Gondwana relative to Laurussia during the Late Paleozoic (Irving, 1977, 2004; Kent & Muttoni, 2020; Muttoni et al., 2003). Although its tectonic accommodation within Pangea remains debated, post-Variscan and pre-Alpine rotations in western Mediterranean blocks, including the Toulon-Cuers Basin and Sardinia, have been interpreted as evidence for intra-Pangea mobility and wrench-related deformation (Aubele et al., 2012, 2014; Kirscher et al., 2011; Siravo et al., 2026). In contrast to these two rigid end-member models, Pastor-Galán (2022) argued that Late Carboniferous–Early Permian Pangea is better regarded as an already amalgamated continental assemblage that still underwent significant internal deformation and relative motion, rather than as a fully rigid supercontinent. This view offers an alternative framework for reconciling the inconsistencies between rigid Pangea A/B end-member models and the available geological and paleomagnetic constraints. Accordingly, we treat the internally deforming early-Pangea scenario proposed by Pastor-Galán (2022) as an important interpretive context for regional paleogeographic relationships, while retaining the reconstruction frameworks of Torsvik et al. (2012) and Huang et al. (2018) as working reference models for inter-block comparison. The compiled data set was then projected into these reference frameworks, and poles from each block were rotated into a common frame anchored at our reference point (33.7°N, 86.7°E), thereby constraining relative paleogeographic positions and enabling assessment of tectonic links and paleogeographic evolution (Figure 3c).

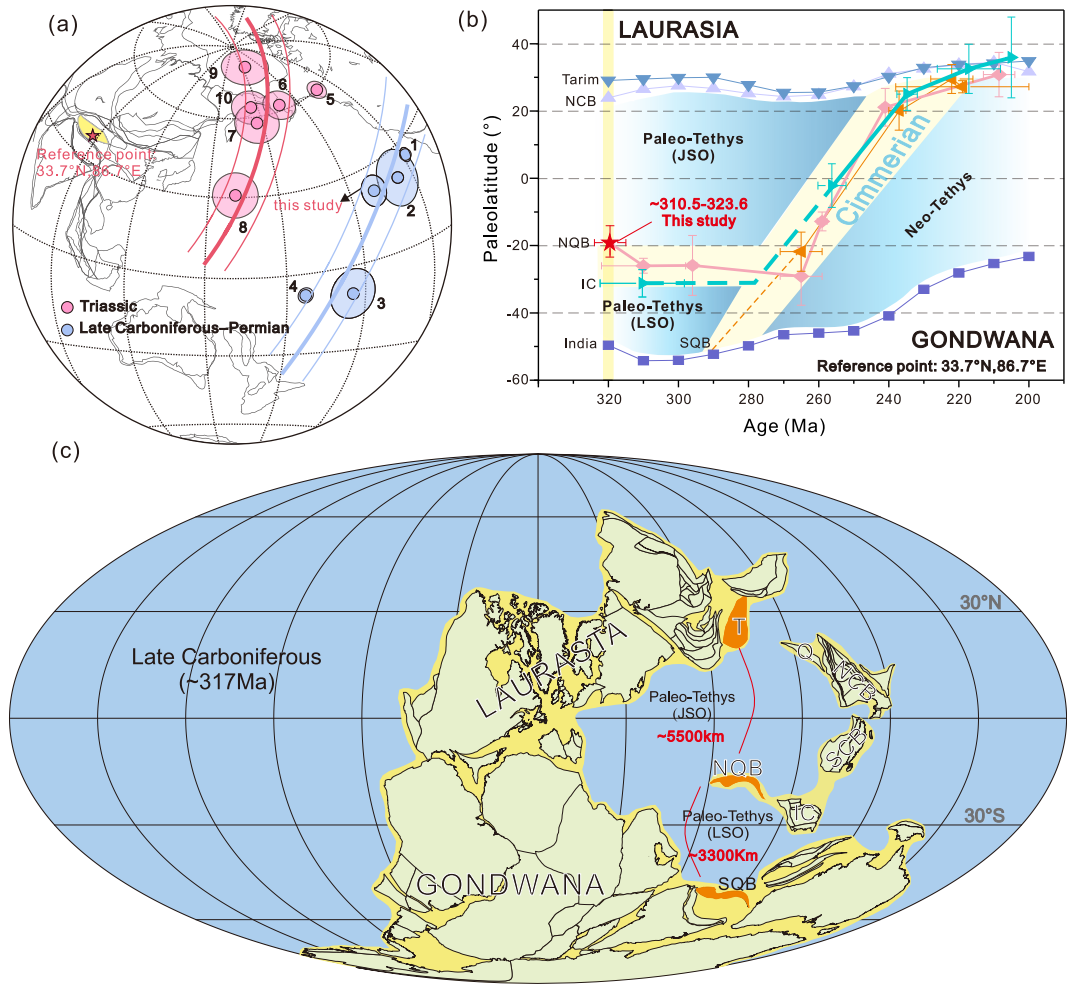

Figure 3. Paleomagnetic poles, paleolatitude evolution, and Late Carboniferous reconstruction of the NQB. (a) Compilation of published paleomagnetic poles for the NQB; circles indicate A_{95}. Pole sources: 1 Yang et al. (2017); 2 Song et al. (2017); 3 Cheng et al. (2024); 4 Ma et al. (2019) and Cheng et al. (2024); 5 Guan, Yan, et al. (2021); 6 Song et al. (2020); 7 Yu et al. (2022); 8 Yu et al. (2025); 9 Zhou et al. (2019); 10 Song et al. (2015). (b) Paleolatitude–time evolution of the NQB and adjacent blocks in the site reference frame; modified after Cheng et al. (2024) and Wei et al. (2025). (c) Late Carboniferous (~317 Ma) paleogeographic reconstruction modified after Huang et al. (2018) and Torsvik et al. (2012). Abbreviations: T = Tarim Block; Q = Qaidam Block; NCB = North China Block; SCB = South China Block; IC = Indochina Block; NQB = North Qiangtang Block; SQB = South Qiangtang Block; JSO = Jinshajiang Ocean; LSO = Longmu Co–Shuanghu Ocean.

The southern margin of the Paleo-Tethys should be evaluated within the broader geological framework of the long-term evolution of the northern Gondwanan passive margin. Studies of the Tethyan Himalaya by Gaetani, Garzanti, and co-workers showed that the northern Indian margin formed part of this passive margin and recorded key stages of Carboniferous–Permian rifting, rift–drift transition, and incipient Neo-Tethyan opening (Gaetani & Garzanti, 1991; Garzanti, 1993a, 1993b, 1999; Garzanti et al., 1996; Sciunnach & Garzanti, 2012). In parallel, Muttoni et al. placed Iran and other Cimmerian blocks along the northern Gondwanan margin prior to their Permian detachment (Muttoni et al., 2003, 2009). For the South Qiangtang Block (SQB), available evidence likewise indicates a clear Gondwanan affinity during the Late Carboniferous–Early Permian: paleomagnetic results suggest that separation from Gondwana likely began in the late Early Permian and was evident by the Middle Permian (Wei et al., 2022, 2023, 2025), whereas glaciogenic deposits, Gondwanan cold-water faunas, Pan-African basement, and Gondwana-derived detrital-zircon populations indicate that the SQB remained attached to the northern Gondwanan margin until at least the late Early Permian (Dong et al., 2011; Liang et al., 1983; Wu et al., 2018; Zhang et al., 2013). Taken together, these observations indicate that, prior to rifting, the Tethyan Himalaya, Iran, the SQB, and other Cimmerian blocks were all situated along the northern

Gondwanan margin on the southern side of the Paleo-Tethys. In the eastern Paleo-Tethyan realm, we therefore use the SQB to constrain the southern margin of the Paleo-Tethys, because it is spatially more directly comparable with the NQB than more distal blocks such as the Tethyan Himalaya or Iran, and thus provides a more regionally appropriate proxy.

However, because robust Late Carboniferous paleomagnetic constraints are still lacking for the SQB, we further used the ∼320 Ma paleomagnetic pole of India as a proxy for the northern Gondwanan margin to estimate the paleoposition of the SQB, with Mayigangri (33.0°N, 88.1°E) as the reference point. This yields an estimated paleolatitude of ∼50.4°S for the SQB.

Meanwhile, the Tarim Block was located at ∼29°N (Huang et al., 2018), close to the Kazakhstan Block. These blocks were probably already amalgamated with Siberia, forming the southern margin of Laurasia (Han et al., 2011; Wang et al., 2007; Zhu et al., 2018). Accordingly, we use Tarim as a regional proxy for the paleolatitude of the southern Laurasian margin, which in turn constrains the northern limit of the Paleo-Tethys Ocean. The South China Block was located near the equator (∼1°S; Huang et al., 2018). In contrast, the North China Block and the Qaidam Block occupied similar paleolatitudes (∼24°N; Figure 3c; Cao et al., 2017; Jiang et al., 2026). Devonian molasse successions, interpreted as post-collisional deposits, are widespread along the northern margin of the Qaidam Block and within the North Qilian Orogenic Belt, indicating that the Qaidam Block and the western margin of the North China Block had most likely already amalgamated by the Devonian (Wu et al., 2025).

Our new Late Carboniferous paleomagnetic results place the NQB at 19.5 ± 5.2°S. A broadly coeval (∼310 Ma) study from the northern slope of the Tanggula Mountains (eastern NQB) yields a paleolatitude of 26.0 ± 2.2°S (Yang et al., 2017). These estimates overlap within uncertainty, indicating that the NQB occupied subtropical latitudes during the Late Carboniferous. Paleontological and sedimentological evidence supports this inference: the fusulinid zonation of the Walongshan Formation correlates with coeval shallow-marine carbonate successions worldwide, consistent with deposition on a tropical–subtropical, shallow-water carbonate platform (Hu et al., 2024; JUIGS, 2006). IC is reconstructed at 31.5 ± 4.0°S (Yan et al., 2020; Figure 3c). Similar Late Carboniferous biostratigraphic assemblages and comparable shallow-marine depositional features in the IC and NQB (Cheng et al., 2024; Wu et al., 2020; Yan et al., 2024) suggest a close paleogeographic affinity between the two blocks. Accordingly, our Late Carboniferous reconstruction places the IC slightly south of, and adjacent to, the NQB (Figure 3c).

6. Geometry of the Paleo-Tethys Ocean

The geometry of the Paleo-Tethys remains debated, with two end-member models: a single oceanic basin along the northern Gondwanan margin (e.g., Golonka & Ford, 2000; Guan, Liu, et al., 2021; Zhang et al., 2022) and a coeval multi-branched system (e.g., Cheng et al., 2024; Wei et al., 2023, 2025; Zhao et al., 2018). Traditional reconstructions generally favored the former for simplicity (e.g., Domeier & Torsvik, 2014; Stampfli & Borel, 2002), treating Iran, Afghanistan, Pamir, Qiangtang, Baoshan, and Simao as blocks attached to northern Gondwana through much of the Paleozoic. Their Late Paleozoic rifting formed the Cimmerian continent, whose northward drift initiated Neo-Tethyan opening and progressive Paleo-Tethyan closure (Muttoni et al., 2003, 2009; Stampfli & Borel, 2002; Şengör, 1984). In this framework, the Paleo-Tethys was viewed as a single basin, whereas intra-oceanic blocks, mélange belts, and back-arc basins were treated as internal complexities rather than distinct branches.

Advances in geology and geochemical constraints, together with refined interpretations of suture-belt origin and tectonic significance, have brought renewed attention to a multi-branched, coeval Paleo-Tethyan oceanic system (Jian et al., 2009; Zhao et al., 2018). The Jinshajiang Ocean contains Middle–Late Paleozoic MOR-type ophiolites and a relatively complete ophiolitic sequence, including mantle peridotite, gabbro, sheeted dike complexes, and pillow basalts (Jian et al., 2009), consistent with formation in a mature oceanic basin. In contrast, the Longmu Co–Shuanghu Ocean preserves Early Paleozoic MOR-type ophiolites (Zhai & Li et al., 2007), Permian ocean-island basalts (Zhai et al., 2006), and Devonian–Triassic deep-marine radiolarian cherts (Li et al., 2008), more consistent with a long-lived oceanic domain that evolved relatively independently. These contrasting records are difficult to reconcile with a single, continuous ocean-basin model by invoking only intra-oceanic structural complexity, and instead provide important geological support for a branched Paleo-Tethys.

Compared with geological approaches alone, paleomagnetism provides quantitative constraints on paleolatitude and therefore offers a measurable basis for evaluating broad paleogeographic relationships among blocks. Against this backdrop, our new paleomagnetic results provide time-anchored constraints on Paleo-Tethyan architecture. Based on the paleolatitude curves (Figure 3b), the paleolatitudinal evolution tracks of the NQB and IC are broadly subparallel from the Late Carboniferous to the Middle Permian (Cheng et al., 2024; Song et al., 2017; Yan et al., 2020, 2024; Yang et al., 2017), implying a possible long-term paleogeographic affinity between the two blocks. Together with the similarity of Carboniferous–Permian sedimentary and paleobiological records between the NQB and IC (Cheng et al., 2024; Yan et al., 2024) and geological evidence for comparable crustal affinity (Wu et al., 2020), we infer that the NQB and IC may have formed a relatively coherent paleogeographic assemblage in the central Paleo-Tethys from the Late Carboniferous to the Middle Permian (Figure 3b). Here, we refer to this inferred assemblage as the NQB–IC central continental domain, which may have acted as a paleogeographic divide between the northern and southern branches of the Paleo-Tethys Ocean (Figure 3c).

On this basis, we quantitatively reconstruct the Late Carboniferous paleogeographic configuration of the Paleo-Tethys Ocean (Figure 3c). We first use the end-member paleolatitudinal separation between the Tarim Block (~30°N) and the SQB (~50°S) to estimate the overall north–south extent of the system, which corresponds to ~8,800 km. Such a large meridional extent implies that the Paleo-Tethys had already developed into a vast, trans-equatorial oceanic basin, plausibly expressed as an eastward-opening, funnel-like seaway. With the NQB–IC central continental domain positioned between the two branches, the paleolatitudinal offset to the SQB (~30°, ~3,300 km) provides a constraint on the width of the southern branch (Longmu Co–Shuanghu Ocean), whereas the offset to the southern margin of Laurasia (~50°, ~5,500 km) constrains the width of the northern branch (Jinshajiang Ocean).

7. Conclusions

This study establishes the first age-anchored Late Carboniferous paleomagnetic constraint for the North Qiangtang Block and provides robust evidence for its Late Carboniferous paleogeographic position in the Southern hemisphere. Combined with regional geological evidence, these results suggest that the Paleo-Tethys had already developed a dual-branch configuration by the Late Carboniferous, with an NQB–IC central continental domain acting as a tectonic divide between a broad northern branch (~5,500 km; Jinshajiang oceanic basin) and a narrower southern branch (~3,300 km; Longmu Co–Shuanghu oceanic basin). This framework provides new constraints on the late Paleozoic tectonic architecture of the eastern Tethyan realm and the evolution of the Paleo-Tethys system.

Conflict of Interest

The authors declare no conflicts of interest relevant to this study.

Availability Statement

Data used in this study (Table S1–S6 in Supporting Information S1) can be accessed at Zenodo (J. Zhang, 2026).

Acknowledgments
Financial support for this study was provided by the National Natural Science Foundation of China (Grants 42488201, 42274097, 42304092, and 42504059) and the Second Tibetan Plateau Scientific Expedition and Research Program (2024QZKK0301). We thank Dr. Yifei Hou, Dr. Min Zhang, Dr. Tingwei Zhang, Dr. Guimei Lu and Dr. Kaixian Qi for their assistance with the laboratory work and manuscript discussion.

References

Angiolini, L., Zanchi, A., Zanchetta, S., Nicora, A., & Vezzoli, G. (2013). The Cimmerian geopuzzle: New data from south Pamir. *Terra Nova*, *25*(5), 352–360. https://doi.org/10.1111/ter.12042

Aubele, K., Bachtadse, V., Muttoni, G., & Ronchi, A. (2014). Paleomagnetic data from late Paleozoic dykes of Sardinia: Evidence for block rotations and implications for the intra-Pangea megashear system. *Geochemistry, Geophysics, Geosystems*, *15*(5), 1684–1697. https://doi.org/10.1002/2014GC005325

Aubele, K., Bachtadse, V., Muttoni, G., Ronchi, A., & Durand, M. (2012). A paleomagnetic study of Permian and Triassic rocks from the Toulon-Cuers Basin, SE France: Evidence for intra-Pangea block rotations in the Permian. *Tectonics*, *31*(3), TC3015. https://doi.org/10.1029/2011TC003026

Cao, Y., Sun, Z. M., Li, H. B., Pei, J. L., Xu, W., Pan, J. W., et al. (2017). New early and late Carboniferous paleomagnetic results from the Qaidam Block, NW China: Implications for the paleogeography of central Asia. *Tectonophysics*, *717*, 242–252. https://doi.org/10.1016/j.tecto.2017.08.014

Cheng, L., Chen, S., Zhang, Y., & Wu, S. (2006). Discovery of Carboniferous strata in northern Qiangtang basin, Tibet. *Earth Science Frontiers*, *13*, 240–243. (In Chinese with English abstract).

Cheng, X., Wei, B. T., Jiang, N., Zhou, Y. N., Kravchinsky, V. A., Chen, Q. L., et al. (2024). Evolution of the North Qiangtang block in the late Paleozoic: Paleomagnetism and its tectonic implications. *GSA Bulletin*, *136*(1–2), 707–724. https://doi.org/10.1130/B36825.1

Cheng, X., Wu, H., Guo, Q., Hou, B., Xia, L., Wang, H., et al. (2012). Paleomagnetic results of late Paleozoic rocks from northern Qiangtang block in Qinghai-Tibet Plateau, China. *Science China Earth Sciences*, *55*(1), 67–75. https://doi.org/10.1007/s11430-011-4287-x

Cheng, X., Wu, H. N., Diao, Z. B., Wang, H. J., Ma, L., Zhang, X. D., et al. (2013). Paleomagnetic data from the late carboniferous–late Permian rocks in eastern Tibet and their implications for tectonic evolution of the northern Qiangtang–Qamdo block. *Science China Earth Sciences*, *56*(7), 1209–1220. https://doi.org/10.1007/s11430-012-4558-1

Cottrell, R. D., Tarduno, J. A., & Roberts, J. (2008). The Kiaman reversed polarity superchron at kiama: Toward a field strength estimate based on single silicate crystals. *Physics of the Earth and Planetary Interiors*, *169*(1–4), 49–58. https://doi.org/10.1016/j.pepi.2008.07.041

Dekkers, M. J. (2012). End-member modelling as an aid to diagnose remagnetization: A brief review. *Geological Society, London, Special Publications*, *371*(1), 253–269. https://doi.org/10.1144/SP371.12

Domeier, M., & Torsvik, T. H. (2014). Plate tectonics in the late Paleozoic. *Geoscience Frontiers*, *5*(3), 303–350. https://doi.org/10.1016/j.gsf.2014.01.002

Domeier, M., Van der Voo, R., & Torsvik, T. H. (2012). Paleomagnetism and Pangea: The road to reconciliation. *Tectonophysics*, *514–517*, 14–43. https://doi.org/10.1016/j.tecto.2011.10.021

Dong, C., Li, C., Wan, Y., Wang, W., Wu, Y., Xie, H., & Liu, D. (2011). Detrital zircon age model of Ordovician Wenquan quartzite south of Lungmuco–Shuanghu suture in the Qiangtang area, Tibet: Constraint on tectonic affinity and source regions. *Science China Earth Sciences*, *54*(7), 1034–1042. https://doi.org/10.1007/s11430-010-4166-x

Elmore, R. D., Muxworthy, A. R., & Aldana, M. (2012). Remagnetization and chemical alteration of sedimentary rocks. *Geological Society*, *371*(1), 1–21. https://doi.org/10.1144/SP371.15

Enkin, R. J. (2003). The direction-correction tilt test: An all-purpose tilt/fold test for paleomagnetic studies. *Earth and Planetary Science Letters*, *212*(1–2), 151–166. https://doi.org/10.1016/S0012-821X(03)00238-3

Fabian, K. (2003). Some additional parameters to estimate domain state from isothermal magnetization measurements. *Earth and Planetary Science Letters*, *213*(3–4), 337–345. https://doi.org/10.1016/S0012-821X(03)00329-7

Fu, Q., Yan, M., Dekkers, M. J., Guan, C., Yu, L., Xu, W., et al. (2022). Remagnetization of the Jurassic limestones in the Zaduo area, eastern Qiangtang terrane (Tibetan Plateau, China): Implications for the India–Eurasia collision. *Geophysical Journal International*, *228*(3), 2073–2091. https://doi.org/10.1093/gji/ggab402

Gaetani, M., & Garzanti, E. (1991). Multicyclic history of the northern India continental margin (Northwestern himalaya). *AAPG Bulletin*, *75*(9), 1427–1446. https://doi.org/10.1306/0C9B2957-1710-11D7-8645000102C1865D

Garzanti, E. (1993a). Himalayan ironstones, "superplumes," and the breakup of Gondwana. *Geology*, *21*(2), 105–108. https://doi.org/10.1130/0091-7613(1993)021<0105:HISATB>2.3.CO;2

Garzanti, E. (1993b). Sedimentary evolution and drowning of a passive margin shelf (Giumal group; Zanskar Tethys Himalaya, India): Palaeoenvironmental changes during final break-up of Gondwanaland. *Geological Society, London, Special Publications*, *74*(1), 277–298. https://doi.org/10.1144/GSL.SP.1993.074.01.20

Garzanti, E. (1999). Stratigraphy and sedimentary history of the Nepal Tethys Himalaya passive margin. *Journal of Asian Earth Sciences*, *17*(5–6), 805–827. https://doi.org/10.1016/S1367-9120(99)00017-6

Garzanti, E., Angiolini, L., & Sciunnach, D. (1996). The mid-Carboniferous to lowermost Permian succession of Spiti (Po group and Ganmachidam formation, Tethys Himalaya, northern India): Gondwana glaciation and rifting of Neo-Tethys. *Geodinamica Acta*, *9*(2), 78–100. https://doi.org/10.1080/09853111.1996.11105279

Golonka, J., & Ford, D. (2000). Pangea (late Carboniferous–Middle Jurassic) paleoenvironment and lithofacies. *Palaeogeography, Palaeoclimatology, Palaeoecology*, *161*(1–2), 1–34. https://doi.org/10.1016/S0031-0182(00)00115-2

Guan, C., Yan, M., Zhang, W., Zhang, D., Fu, Q., Yu, L., et al. (2021). Paleomagnetic and chronologic data bearing on the Permian/Triassic boundary position of Qamdo in the eastern Qiangtang terrane: Implications for the closure of the Paleo-Tethys. *Geophysical Research Letters*, *48*(6), e2020GL092059. https://doi.org/10.1029/2020GL092059

Guan, Q., Liu, Y., Neubauer, F., Li, S., Genser, J., Yuan, S., et al. (2021). Opening of the West Paleo-Tethys Ocean: New insights from earliest Devonian meta-mafic rocks in the Saualpe crystalline basement, Eastern Alps. *Gondwana Research*, *97*, 121–137. https://doi.org/10.1016/j.gr.2021.05.017

Han, B., He, G., Wang, X., & Guo, Z. (2011). Late Carboniferous collision between the Tarim and Kazakhstan–Yili terranes in the western segment of the South Tian Shan Orogen, Central Asia, and implications for the Northern Xinjiang, western China. *Earth-Science Reviews*, *109*(3–4), 74–93. https://doi.org/10.1016/j.earscirev.2011.09.001

Hu, K., Wang, X., Wang, W., Song, Y., Ye, X., Li, L., et al. (2024). Carboniferous integrative stratigraphy, biotas, and paleogeographical evolution of the Qinghai-Tibetan Plateau and its surrounding areas. *Science China Earth Sciences*, *67*(4), 1071–1106. https://doi.org/10.1007/s11430-023-1150-0

Huang, B., Yan, Y., Piper, J. D. A., Zhang, D., Yi, Z., Yu, S., & Zhou, T. (2018). Paleomagnetic constraints on the paleogeography of the East Asian blocks during Late Paleozoic and early Mesozoic times. *Earth-Science Reviews*, *186*, 8–36. https://doi.org/10.1016/j.earscirev.2018.02.004

Irving, E. (1977). Drift of the major continental blocks since the Devonian. *Nature*, *270*(5635), 304–309. https://doi.org/10.1038/270304a0

Irving, E. (2004). The case for Pangea B, and the intra-Pangean megashear. In J. E. T. Channell, D. V. Kent, W. Lowrie, & J. G. Meert (Eds.), *Timescales of the paleomagnetic field* (Vol. 145, pp. 13–27). Geophysical Monograph Series. https://doi.org/10.1029/145GM02

Jackson, M. J., & Swanson-Hysell, N. L. (2012). Rock magnetism of remagnetized carbonate rocks: Another look. *Geological Society*, *371*, 229–251. https://doi.org/10.1144/SP371.3

Jian, P., Liu, D., Kröner, A., Zhang, Q., Wang, Y., Sun, X., & Zhang, W. (2009). Devonian to Permian plate tectonic cycle of the Paleo-Tethys Orogen in southwest China (I): Geochemistry of ophiolites, arc/back-arc assemblages and within-plate igneous rocks. *Lithos*, *113*(3–4), 748–766. https://doi.org/10.1016/j.lithos.2009.04.004

Jiang, N., Cheng, X., Wei, B., Xing, L., Zhang, J., Zhang, D., et al. (2026). New late Carboniferous paleomagnetic results from the Qaidam Block: Constraints on the ocean–continent configuration of the Paleo-Tethyan realm. *Science China Earth Sciences*. https://doi.org/10.1360/SSTe-2025-0264

Jiang, N., Wu, H., Li, Y., Wei, B., Zhou, Y., Zhang, W., et al. (2022). Preliminary paleomagnetic results of the Early–Middle Silurian rocks from North Qiangtang Terrane, and its tectonic implications. *Chinese Journal of Geophysics*, *65*(3), 1057–1070. https://doi.org/10.6038/cjg2022P0065

Jilin University Institute of Geological Survey (JUIGS). (2006). *Regional geological survey report of the people's Republic of China (April)*. Jilin University Institute of Geological Survey. (In Chinese).

Kapp, P., Yin, A., Manning, C. E., Harrison, T. M., Taylor, M. H., & Ding, L. (2003). Tectonic evolution of the early Mesozoic blueschist-bearing Qiangtang metamorphic belt, central Tibet. *Tectonics*, *22*(4), 1043. https://doi.org/10.1029/2002TC001383

Kent, D. V., & Muttoni, G. (2020). Pangea B and the late Paleozoic ice Age. *Palaeogeography, Palaeoclimatology, Palaeoecology*, *553*, 109753. https://doi.org/10.1016/j.palaeo.2020.109753

Kirscher, U., Aubele, K., Muttoni, G., Ronchi, A., & Bachtadse, V. (2011). Paleomagnetism of Jurassic carbonate rocks from Sardinia: No indication of post-Jurassic internal block rotations. *Journal of Geophysical Research*, *116*(B12), B12107. https://doi.org/10.1029/2011JB008422

Li, C. (2008). Longmu Co–Shuanghu–Lancang River suture zone in the Qinghai–Tibet Plateau: A review on 20 years of study. *Geological Review*, *54*(1), 105–119.

Liang, D., Nie, Z., Guo, T., Xu, B., & Zhang, Y. (1983). Permo–Carboniferous gondwana–tethys facies in southern Karakoran Ali, Xizang (Tibet). *Earth Science*, *19*, 9–27. (In Chinese with English abstract).

Lin, J., & Watts, D. R. (1988). Palaeomagnetic results from the Tibetan Plateau. *Philosophical Transactions of the Royal Society of London. Series A, Mathematical and Physical Sciences*, *327*(1594), 239–262. https://doi.org/10.1098/rsta.1988.0128

Ma, X., Li, Y., Tan, X., Li, S., Li, Z., Zhang, J., et al. (2024). Late Triassic paleolatitude of the Southern Qiangtang terrane, central Tibet: Implications for the closure of the Longmu Co–Shuanghu Paleo-Tethyan Ocean. *Journal of Asian Earth Sciences*, *269*, 106174. https://doi.org/10.1016/j.jseaes.2024.106174

Ma, X., Tan, X., Li, Y., Wang, C., Han, Z., Li, S., et al. (2025). Initial closure of the Longmu Co–Shuanghu Paleo-Tethyan Ocean: Constraints based on new paleomagnetic data from the Middle Triassic volcanic-sedimentary sequence, southern Qiangtang terrane. *Tectonics*, *44*(1), e2024TC008504. https://doi.org/10.1029/2024TC008504

Ma, Y., Hu, S., Dekkers, M. J., Yang, T., Niu, C., & Wang, H. (2025). An updated inclination-only fold test for paleomagnetic studies. *Tectonophysics*, *912*, 230854. https://doi.org/10.1016/j.tecto.2025.230854

Ma, Y., Wang, Q., Wang, J., Yang, T., Tan, X., Dan, W., et al. (2019). Paleomagnetic constraints on the origin and drift history of the North Qiangtang Terrane in the Late Paleozoic. *Geophysical Research Letters*, *46*(2), 689–697. https://doi.org/10.1029/2018GL080964

McElhinny, M. W. (1964). Statistical significance of the fold test in palaeomagnetism. *Geophysical Journal International*, *8*(3), 338–340. https://doi.org/10.1111/j.1365-246X.1964.tb06300.x

McFadden, P. L. (1990). A new fold test for palaeomagnetic studies. *Geophysical Journal International*, *103*(1), 163–169. https://doi.org/10.1111/j.1365-246X.1990.tb01761.x

Meert, J. G., Pivarunas, A. F., Evans, D. A. D., Pisarevsky, S. A., Pesonen, L. J., Li, Z.-X., et al. (2020). The magnificent seven: A proposal for modest revision of the Van der Voo (1990) quality index. *Tectonophysics*, *790*, 228549. https://doi.org/10.1016/j.tecto.2020.228549

Muttoni, G., Kent, D. V., Garzanti, E., Brack, P., Abrahamsen, N., & Gaetani, M. (2003). Early Permian pangea "B" to Late Permian Pangea A. *Earth and Planetary Science Letters*, *215*(3–4), 379–394. https://doi.org/10.1016/S0012-821X(03)00452-7

Muttoni, G., Mattei, M., Balini, M., Zanchi, A., Gaetani, M., & Berra, F. (2009). The drift history of Iran from the Ordovician to the Triassic. *Geological Society*, *312*, 7–29. https://doi.org/10.1144/SP312.2

Pastor-Galán, D. (2022). From supercontinent to superplate: Late Paleozoic Pangea's inner deformation suggests it was a short-lived superplate. *Earth-Science Reviews*, *226*, 103918. https://doi.org/10.1016/j.earscirev.2022.103918

Pastor-Galán, D., Dekkers, M. J., Gutiérrez-Alonso, G., Brouwer, D., Groenewegen, T., Krijgsman, W., et al. (2016). Paleomagnetism of the Central Iberian curve's putative hinge: Too many oroclines in the Iberian Variscides. *Gondwana Research*, *39*, 96–113. https://doi.org/10.1016/j.gr.2016.06.016

Pastor-Galán, D., López-Carmona, A., Rezaeian, M., Tsujimori, T., Gutiérrez-Alonso, G., Yi, K., & Langereis, C. (2025). From Rheic to paleotethys: Subduction history of the Shanderman eclogites (NW Iran). *GSA Bulletin*, *137*(9–10), 4478–4496. https://doi.org/10.1130/B38187.1

Pullen, A., Kapp, P., Gehrels, G. E., Vervoort, J. D., & Ding, L. (2008). Triassic continental subduction in central Tibet and Mediterranean-style closure of the Paleo-Tethys Ocean. *Geology*, *36*(5), 351–354. https://doi.org/10.1130/G24435A.1

Sciunnach, D., & Garzanti, E. (2012). Subsidence history of the Tethys Himalaya. *Earth-Science Reviews*, *111*(1–2), 179–198. https://doi.org/10.1016/j.earscirev.2011.11.007

Şengör, A. C. (1984). *The Cimmeride orogenic system and the tectonics of Eurasia* (Vol. 195, pp. 1–82). Geological Society of America Special Paper.

Siravo, G., Speranza, F., Oggiano, G., & Spagnuolo, L. (2026). Post-Eocene 90° CCW rotation of Sardinia-South Corsica: Paleomagnetic evidence from Permian-Cretaceous sediments of Nurra (NW Sardinia). *Tectonics*, *45*(5), e2026TC009397. https://doi.org/10.1029/2026TC009397

Song, C., Wang, J., Fu, X. G., Feng, X. L., Chen, M., & He, L. (2012). Late Triassic paleomagnetic data from the Qiangtang terrane of Tibetan Plateau and their tectonic significances. *Journal of Jilin University (Earth Science Edition)*, *42*(2), 526–535. (In Chinese with English abstract).

Song, P., Ding, L., Li, Z., Lippert, P. C., Yang, T., Zhao, X., et al. (2015). Late Triassic paleolatitude of the Qiangtang block: Implications for the closure of the Paleo-Tethys Ocean. *Earth and Planetary Science Letters*, *424*, 69–83. https://doi.org/10.1016/j.epsl.2015.05.020

Song, P., Ding, L., Li, Z., Lippert, P. C., & Yue, Y. (2017). An early bird from Gondwana: Paleomagnetism of Lower Permian lavas from northern Qiangtang (Tibet) and the geography of the Paleo-Tethys. *Earth and Planetary Science Letters*, *475*, 119–133. https://doi.org/10.1016/j.epsl.2017.07.023

Song, P., Ding, L., Lippert, P. C., Li, Z., Zhang, L., & Xie, J. (2020). Paleomagnetism of Middle Triassic lavas from northern Qiangtang (Tibet): Constraints on the closure of the Paleo-Tethys Ocean. *Journal of Geophysical Research: Solid Earth*, *125*(2), e2019JB017804. https://doi.org/10.1029/2019JB017804

Stampfli, G. M., & Borel, G. D. (2002). A plate tectonic model for the Paleozoic and Mesozoic constrained by dynamic plate boundaries and restored synthetic oceanic isochrons. *Earth and Planetary Science Letters*, *196*(1–2), 17–33. https://doi.org/10.1016/S0012-821X(01)00588-X

Tauxe, L., Gee, J. S., Li, Y., Pick, T., Jin, J., Swanson-Hysell, N. L., et al. (2016). PmagPy: Software package for paleomagnetic data analysis and a bridge to the magnetics information consortium (MagIC) database. *Geochemistry, Geophysics, Geosystems*, *17*(6), 2450–2463. https://doi.org/10.1002/2016GC006307

Torsvik, T. H., & Cocks, L. R. M. (2017). *Earth history and palaeogeography*. Cambridge University Press.

Torsvik, T. H., Van der Voo, R., Preeden, U., Mac Niocaill, C., Steinberger, B., Doubrovine, P. V., et al. (2012). Phanerozoic polar wander, palaeogeography and dynamics. *Earth-Science Reviews*, *114*(3–4), 325–368. https://doi.org/10.1016/j.earscirev.2012.06.007

Vaes, B., van Hinsbergen, D. J. J., van de Lagemaat, S. H. A., van der Wiel, E., Lom, N., Advokaat, E. L., et al. (2023). A global apparent polar wander path for the last 320 Ma calculated from site-level paleomagnetic data. *Earth-Science Reviews*, *245*, 104547. https://doi.org/10.1016/j.earscirev.2023.104547

Wang, B., Chen, Y., Zhan, S., Shu, L. S., Faure, M., Cluzel, D., et al. (2007). Primary Carboniferous and Permian paleomagnetic results from the Yili Block (NW China) and their implications on the geodynamic evolution of Chinese Tianshan Belt. *Earth and Planetary Science Letters*, *263*(3–4), 288–308. https://doi.org/10.1016/j.epsl.2007.08.037

Wang, Y., Qian, X., Cawood, P. A., Liu, H., Feng, Q., Zhao, G., et al. (2018). Closure of the East Paleotethyan Ocean and amalgamation of the Eastern cimmerian and southeast Asia continental fragments. *Earth-Science Reviews*, *186*, 195–230. https://doi.org/10.1016/j.earscirev.2017.09.013

Watson, G. S., & Enkin, R. J. (1993). The fold test in paleomagnetism as a parameter estimation problem. *Geophysical Research Letters*, *20*(19), 2135–2137. https://doi.org/10.1029/93GL01901

Wei, B., Cheng, X., Domeier, M., Jiang, N., Wu, Y., Zhang, W., et al. (2022). Placing another piece of the Tethyan puzzle: The first Paleozoic paleomagnetic data from the South Qiangtang block and its paleogeographic implications. *Tectonics*, *41*(10), e2022TC007355. https://doi.org/10.1029/2022TC007355

Wei, B., Cheng, X., Domeier, M., Yang, P., Li, S., Xing, L., et al. (2025). A Cimmerian keystone: Middle–late Triassic paleomagnetic and calcite geochronologic constraints on the South Qiangtang Block. *Earth and Planetary Science Letters*, *664*, 119442. https://doi.org/10.1016/j.epsl.2025.119442

Wei, B., Cheng, X., Domeier, M., Zhou, Y., Chen, Q., Jiang, N., et al. (2023). Paleomagnetism of Late Triassic volcanic rocks from the South Qiangtang Block, Tibet: Constraints on Longmu Co–Shuanghu Ocean closure in the Paleo-Tethys realm. *Geophysical Research Letters*, *50*(19), e2023GL104759. https://doi.org/10.1029/2023GL104759

Wu, C., Zhao, Y., Li, J., Liu, W., Zuza, A. V., Haproff, P. J., & Ding, L. (2025). Multicyclic Phanerozoic orogeny recorded in the Qaidam continent, northern Tibet: Implications for the tectonic evolution of the Tethyan orogenic system. *GSA Bulletin*, *137*(3–4), 1553–1581. https://doi.org/10.1130/B37906.1

Wu, F., Wan, B., Zhao, L., Xiao, W., & Zhu, R. (2020). Tethyan geodynamics. *Acta Petrologica Sinica*, *36*, 1627–1674. (In Chinese with English abstract).

Wu, L., Yuan, T., Jin, H., & Liu, Y. (2018). Petrology of low-grade metamorphic quartz sandstones within northwestern Tibetan regions: Implications to the tectonic evolution of the northwestern Tibet. *Acta Petrologica Sinica*, *34*, 701–718. (In Chinese with English abstract).

Xie, C., Shi, Z., Duan, M., Chen, H., Xu, M., Bai, X., & Zhang, J. (2025). Research progress and existing issues on the Paleozoic strata in the Qiangtang Terrane of the Qinghai-Xizang Plateau. *Journal of Northwest University*, *55*(3), 501–522. https://doi.org/10.16152/j.cnki.xdxbzr.2025-03-003

Xu, Y., Yang, Z., Tong, Y. B., Wang, H., Gao, L., & An, C. (2015). Further paleomagnetic results for Lower Permian basalts of the Baoshan Terrane, southwestern China, and paleogeographic implications. *Journal of Asian Earth Sciences*, *104*, 99–114. https://doi.org/10.1016/j.jseaes.2014.10.029

Yan, Y., Duan, L., Liang, S., Wang, J., Huang, B., Zheng, W., & Zhang, P. (2020). Paleomagnetic constraint on the Carboniferous paleoposition of Indochina and its implications for the evolution of eastern Paleo-Tethys Ocean. *Tectonics*, *39*(7), e2020TC006168. https://doi.org/10.1029/2020TC006168

Yan, Y., Huang, B., Zhang, P., Zhao, J., Zhang, D., Jia, S., et al. (2024). Paleomagnetic constraint on the movement of the Indochina Block since late Paleozoic: Progress and prospect. *Chinese Science Bulletin*, *69*(18), 2498–2517. https://doi.org/10.1360/TB-2023-0884

Yang, X., Cheng, X., Zhou, Y., Ma, L., Zhang, X., Yan, Z., et al. (2017). Paleomagnetic results from late Carboniferous to early Permian rocks in the northern Qiangtang terrane, Tibet, China, and their tectonic implications. *Science China Earth Sciences*, *60*(1), 124–134. https://doi.org/10.1007/s11430-015-5462-7

Yao, Y., Huang, W., Qin, H., Bian, W., Jia, Z., & Deng, C. (2024). Remagnetization of Upper Triassic limestone from the central Lhasa terrane (Tibet): Identification, mechanisms, and implications for diagnosing secondary remanent magnetization in carbonate rocks. *Journal of Geophysical Research: Solid Earth*, *129*(7), e2024JB029316. https://doi.org/10.1029/2024JB029316

Yu, L., Yan, M., Domeier, M., Guan, C., Shen, M., Fu, Q., et al. (2022). New paleomagnetic and chronological constraints on the Late Triassic position of the Eastern Qiangtang Terrane: Implications for the closure of the Paleo-Jinshajiang Ocean. *Geophysical Research Letters*, *49*(2), e2021GL096902. https://doi.org/10.1029/2021GL096902

Yu, L., Yan, M., Domeier, M., Li, B., Shen, M., Guan, C., et al. (2025). New paleomagnetic results from Late Triassic limestone of the Eastern Qiangtang Terrane: Implications for the closure of the Paleo-Jinshajiang Ocean. *Palaeogeography, Palaeoclimatology, Palaeoecology*, *657*, 112610. https://doi.org/10.1016/j.palaeo.2024.112610

Zhai, Q., Jahn, B. M., Zhang, R., Wang, J., & Su, L. (2011). Triassic subduction of the Paleo-Tethys in northern Tibet, China: Evidence from the geochemical and isotopic characteristics of eclogites and blueschists of the Qiangtang block. *Journal of Asian Earth Sciences*, *42*(6), 1356–1370. https://doi.org/10.1016/j.jseaes.2011.07.023

Zhai, Q., & Li, C. (2007). Zircon SHRIMP dating of volcanic rock from the Nadigangri formation in Juhuashan, Qiangtang, northern Tibet and its geological significance. *Acta Geologica Sinica*, *81*, 795–800. (In Chinese with English abstract).

Zhai, Q., Li, C., & Huang, X. (2006). Geochemistry of Permian basalt in the Jiaomuri area, central Qiangtang, Tibet, China, and its tectonic significance. *Geological Bulletin of China*, *25*(12), 1419–1427. (In Chinese with English abstract).

Zhang, J. (2026). Late Carboniferous paleomagnetism from North Qiangtang block reveals a multibranched paleo-tethys Ocean. *Zenodo*. [Dataset]. https://doi.org/10.5281/zenodo.20279030

Zhang, S., Li, Y., Wu, G., & Ji, Z. (2021). Corals of the upper Carboniferous Walongshan formation in north qiangtang block. *Geological Review*, *67*, 249–250. https://doi.org/10.16509/j.georeview.2021.s1.110

Zhang, Y., Shen, S., Zhai, Q., Zhang, Y., & Yuan, D. (2016). Discovery of a Sphaeroschwagerina fusuline fauna from the Raggyorcaka Lake area, northern Tibet: Implications for the origin of the Qiangtang Metamorphic Belt. *Geological Magazine*, *153*(3), 537–543. https://doi.org/10.1017/S0016756815000795

Zhang, Y., Shi, G., & Shen, S. (2013). A review of Permian stratigraphy, palaeobiogeography and palaeogeography of the Qinghai–Tibet Plateau. *Gondwana Research*, *24*(1), 55–76. https://doi.org/10.1016/j.gr.2012.06.010

Zhang, Y., Zheng, B., Wang, J., & Fu, X. (2022). Locating northern Qiangtang on the margin of Gondwana or Laurasia? Evidence from detrital zircon geochronology. *Journal of Asian Earth Sciences*, *237*, 105343. https://doi.org/10.1016/j.jseaes.2022.105343

Zhao, G., Wang, Y., Huang, B., Dong, Y., Li, S., Zhang, G., & Yu, S. (2018). Geological reconstructions of the East Asian blocks: From the breakup of Rodinia to the assembly of Pangea. *Earth-Science Reviews*, *186*, 262–286. https://doi.org/10.1016/j.earscirev.2018.10.003

Zhou, Y., Cheng, X., Wu, Y., Kravchinsky, V., Shao, R., Zhang, W., et al. (2019). The northern Qiangtang Block rapid drift during the Triassic period: Paleomagnetic evidence. *Geoscience Frontiers*, *10*(6), 2313–2327. https://doi.org/10.1016/j.gsf.2019.05.003

Zhu, R., Zhao, P., & Zhao, L. (2022). Tectonic evolution and geodynamics of the Neo-Tethys Ocean. *Science China Earth Sciences*, *65*, 1–24. https://doi.org/10.1007/s11430-021-9845-7

Zhu, X., Wang, B., Chen, Y., Liu, H., Horng, C.-S., Choulet, F., et al. (2018). First early Permian paleomagnetic pole for the Yili Block and its implications for late Paleozoic postorogenic kinematic evolution of the SW Central Asian Orogenic Belt. *Tectonics*, *37*(6), 1709–1732. https://doi.org/10.1029/2017TC004642

References From the Supporting Information

Cogné, J.-P. (2003). PaleoMac: A macintosh™ application for treating paleomagnetic data and making plate reconstructions. *Geochemistry, Geophysics, Geosystems*, *4*(1), 1007. https://doi.org/10.1029/2001GC000227

Coward, M. P., Kidd, W. S. F., Pan, Y., Shackleton, R. M., & Zhang, H. (1988). The structure of the 1985 Tibet Geotraverse, Lhasa to Golmud. *Philosophical Transactions of the Royal Society of London. Series A, Mathematical and Physical Sciences*, *327*(1594), 307–336. https://doi.org/10.1098/rsta.1988.0131

Dunlop, D. J. (2002). Theory and application of the Day plot (Mrs/Ms versus Hcr/Hc) 2. Application to data for rocks, sediments, and soils. *Journal of Geophysical Research*, *107*(B3), 2057. https://doi.org/10.1029/2001JB000487

Enkin, R. J. (1994). *A computer program package for analysis and presentation of paleomagnetic data (Pacific geoscience Centre, Geological Survey of Canada Report 16* (pp. 1–16). Geological Survey of Canada.

Hill, C. A., Polyak, V. J., Asmerom, Y., & Provencio, P. (2016). Constraints on a Late Cretaceous uplift, denudation, and incision of the Grand Canyon region, southwestern Colorado Plateau, USA, from U–Pb dating of lacustrine limestone. *Tectonics*, *35*(4), 896–906. https://doi.org/10.1002/2016TC004166

Hodych, J. P., & Buchan, K. L. (1994). Early Silurian palaeolatitude of the Springdale Group redbeds of central Newfoundland: A palaeomagnetic determination with a remanence anisotropy test for inclination error. *Geophysical Journal International*, *117*(3), 640–652. https://doi.org/10.1111/j.1365-246x.1994.tb02459.x

Kapp, P., Yin, A., Harrison, T. M., & Ding, L. (2005). Cretaceous-Tertiary shortening, basin development, and volcanism in central Tibet. *GSA Bulletin*, *117*(7–8), 865–878. https://doi.org/10.1130/B25595.1

Kodama, K. P. (2012). *Paleomagnetism of sedimentary rocks: Process and interpretation*. Wiley-Blackwell. https://doi.org/10.1002/9781118384138

Koymans, M. R., Langereis, C. G., Pastor-Galán, D., & van Hinsbergen, D. J. J. (2016). Paleomagnetism.org: An online multi-platform open source environment for paleomagnetic data analysis. *Computers & Geosciences*, *93*, 127–137. https://doi.org/10.1016/j.cageo.2016.05.007

Koymans, M. R., van Hinsbergen, D. J. J., Pastor-Galán, D., Vaes, B., & Langereis, C. G. (2020). Towards FAIR paleomagnetic data management through Paleomagnetism.org 2.0. *Geochemistry, Geophysics, Geosystems*, *21*(2), e2019GC008838. https://doi.org/10.1029/2019GC008838

Paton, C., Hellstrom, J., Paul, B., Woodhead, J., & Hergt, J. (2011). Iolite: Freeware for the visualisation and processing of mass spectrometric data. *Journal of Analytical Atomic Spectrometry*, *26*(12), 2508–2518. https://doi.org/10.1039/C1JA10172B

Tauxe, L., Kodama, K. P., & Kent, D. V. (2008). Testing corrections for paleomagnetic inclination error in sedimentary rocks: A comparative approach. *Physics of the Earth and Planetary Interiors*, *169*(1–4), 152–165. https://doi.org/10.1016/j.pepi.2008.05.006

van Hinsbergen, D. J. J., Kapp, P., Dupont-Nivet, G., Lippert, P. C., DeCelles, P. G., & Torsvik, T. H. (2011). Restoration of Cenozoic deformation in Asia and the size of Greater India. *Tectonics*, *30*(5), TC5003. https://doi.org/10.1029/2011TC002908

Vermeesch, P. (2018). IsoplotR: A free and open toolbox for geochronology. *Geoscience Frontiers*, *9*(5), 1479–1493. https://doi.org/10.1016/j.gsf.2018.04.001

Wang, T., Yang, P., He, S., Hoffmann, R., Zhang, Q., Farnsworth, A., et al. (2024). Absolute age and temperature of belemnite rostra: Constraints on the Early Cretaceous cooling event. *Global and Planetary Change*, *233*, 104353. https://doi.org/10.1016/j.gloplacha.2023.104353

Yang, P., Ren, Z., Nuriel, P., Nguyen, A. D., Feng, Y. X., Zhou, R., & Zhao, J. X. (2024). Cenozoic faulting leading to petroleum escape in SW Ordos Basin, China: Evidence from fault-related calcite in situ U–Pb dating, rare earth elements and fluid inclusions. *Marine and Petroleum Geology*, *170*, 107071. https://doi.org/10.1016/j.marpetgeo.2024.107071